

13 Feb 1995

Composition Profiles in Electrodeposited Ceramic Superlattices

Jay A. Switzer

Missouri University of Science and Technology, jswitzer@mst.edu

Richard J. Phillips

Teresa D. Golden

Follow this and additional works at: https://scholarsmine.mst.edu/chem_facwork

 Part of the [Chemistry Commons](#)

Recommended Citation

J. A. Switzer et al., "Composition Profiles in Electrodeposited Ceramic Superlattices," *Applied Physics Letters*, vol. 66, no. 7, pp. 819-821, American Institute of Physics (AIP), Feb 1995.

The definitive version is available at <https://doi.org/10.1063/1.113432>

This Article - Journal is brought to you for free and open access by Scholars' Mine. It has been accepted for inclusion in Chemistry Faculty Research & Creative Works by an authorized administrator of Scholars' Mine. This work is protected by U. S. Copyright Law. Unauthorized use including reproduction for redistribution requires the permission of the copyright holder. For more information, please contact scholarsmine@mst.edu.

Composition profiles in electrodeposited ceramic superlattices

Jay A. Switzer,^{a)} Richard J. Phillips, and Teresa D. Golden

University of Missouri-Rolla, Graduate Center for Materials Research, Rolla, Missouri 65401

(Received 28 September 1994; accepted for publication 5 December 1994)

Superlattices in the Pb–Tl–O system with layer thicknesses in the 4–6 nm range were electrodeposited from a single aqueous solution by pulsing the applied potential during deposition. The current-time transients that resulted from the potential steps were monitored to both calculate and tailor the composition profiles of the superlattices during growth. The Cottrell method was used to determine that Tl(I) oxidation was diffusion limited at high potentials. The diffusion limitation resulted in a composition profile that was graded throughout the layer with a $t^{-1/2}$ dependence. Superlattices grown at lower potentials in which both reactants were under kinetic control had square composition profiles. © 1995 American Institute of Physics.

Superlattices of ceramics^{1–5} and metals^{6–9} can be electrodeposited from a single aqueous plating solution by pulsing the applied potential or current during deposition. There are several possible advantages to the electrochemical method for depositing nanometer-scale layered materials. The low processing temperatures (room temperature in our work) minimize interdiffusion, layer thicknesses can be designed by selecting the appropriate current and dwell time, composition and defect chemistry can be controlled,⁵ films can be deposited onto complex shapes, the driving force can be precisely controlled, and the technique is not capital intensive.

There is an additional advantage of the electrochemical method which has not been sufficiently exploited. The current-time transient following a potential step provides an *in situ* measure of the deposition process, since the current is proportional to the deposition rate. In this letter, we use the current-time transients which result from pulsed potential deposition to both calculate and tailor the composition profile in the layers of electrodeposited superlattices in the Pb–Ti–O system. Earlier work by scanning tunneling microscopy (STM) has shown that the apparent height profiles in cross sections of superlattices grown under potential control were more square than those of superlattices grown under current control.^{2,3} The x-ray patterns of the potential controlled samples had x-ray superlattice satellites out to fourth order.² Although these are qualitative measures of the composition profile obtained *after* deposition of the superlattices, in the present work we use current-time transients to quantify the composition profiles *during* deposition.

The solution used to grow the superlattices in this study was 0.005 M TlNO₃ and 0.1 M Pb(NO₃)₂ in 5 M NaOH (**Caution:** thallium and lead compounds are extremely toxic). At low potentials such as 70 mV versus the saturated calomel electrode (SCE) the observed current density was 0.05 mA/cm², the deposition rate was 0.06 nm/s, and the composition of the bulk film was 45 at. % lead on a metals-only basis. At this potential, the deposition is kinetically controlled in both thallium and lead. For an electrochemical reaction the rate is exponentially related to potential in the activation region. As the potential is increased the lead con-

tent of the film increases as the deposition becomes mass-transport limited in Tl(I). At 230 mV versus SCE the current density and deposition rate were 4.6 mA/cm² and 5 nm/s, respectively, and the composition was 76 at. % lead. All of the oxides in this study had a fcc fluorite structure with a strong [210] texture.¹⁰ X-ray diffraction was used to verify that the layered structures were superlattices.¹ The modulation wavelengths from the high angle x-ray satellite spacings were in good agreement with those calculated from Faraday's law.

Superlattices were grown by pulsing between 70 and 230 mV versus SCE. The applied square waveform and resulting current-time transient are shown in Fig. 1. The current was relatively constant during the 70 mV pulse, suggesting that the composition profile is also flat during this pulse. We attribute the initial decay and rising portions of the 230 mV

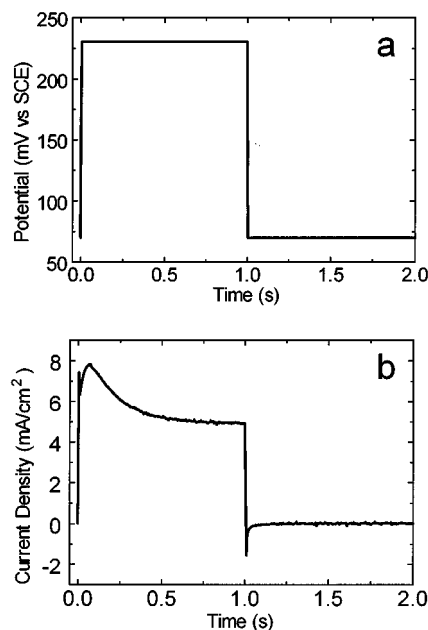


FIG. 1. Applied potential-time waveform (a) and resulting current time transient (b) for the electrodeposition of a Pb–Tl–O superlattice. The potential was pulsed between 70 and 230 mV vs SCE in a stirred solution of 0.005 M TlNO₃ and 0.1 M Pb(NO₃)₂ in 5 M NaOH. The modulation wavelength is 10 nm. The 70 mV layer is 4 nm thick and the 230 mV layer is 6 nm thick.

^{a)}Electronic mail: SWITZ@umrvmb.umr.edu

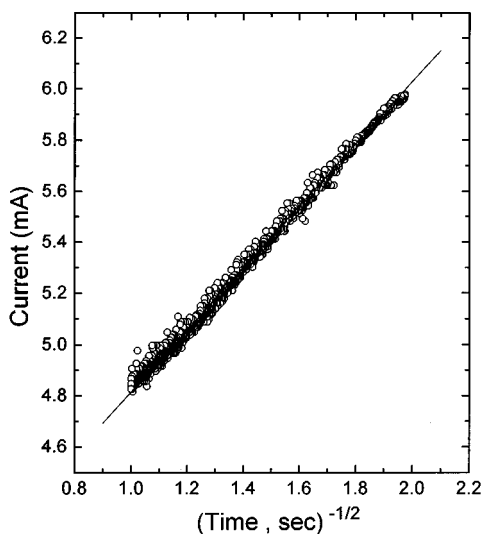


FIG. 2. Cottrell plot of current vs $(\text{time})^{-1/2}$ for the 230 mV transient from Fig. 1. The slope of the plot identifies Tl(I) as the diffusion-limited species.

current-time transient up to 0.14 s to double layer charging and two-dimensional growth, respectively. During this time, the Faradaic thickness of the deposit is approximately 0.6 nm. We do not attempt to calculate the composition profile during this early segment of the 230 mV pulse. A plot of $\log(\text{current})$ versus $\log(\text{time})$ during the segment between 0.14 and 1.0 s (0.6–6.4 nm) had a slope of -0.494 ± 0.001 . The $t^{-1/2}$ dependence of the current in this region is consistent with diffusion limitation of the current. The identity of the diffusion-limiting component can be determined by applying the Cottrell equation to the current-time decay. The Cottrell equation is

$$i = nFAD^{1/2}C^* \pi^{-1/2} t^{-1/2},$$

where n is the number of electrons transferred, F is Faraday's number, A is the electrode area (1 cm^2 in our studies), D is the diffusion coefficient, C^* is the bulk concentration for the diffusion limited component, and t is the time.¹¹

A Cottrell plot for the 230 mV pulse is shown in Fig. 2. The slope of the line in Fig. 2 of $0.77 \text{ mA s}^{1/2}$ is in good agreement with a slope of $0.79 \text{ mA s}^{1/2}$ that is observed in a solution of only 0.005 M TlNO_3 . For comparison, the Cottrell slope observed in a solution of 0.1 M $\text{Pb}(\text{NO}_3)_2$ was $6.7 \text{ mA s}^{1/2}$. These results are consistent with Tl(I) being the diffusion-limited species at this potential. This is the expected result, since the concentration of Tl(I) is low relative to the concentration of Pb(II), and the applied potential of 230 mV provides a low driving force for Pb(II) oxidation and a high driving force for Tl(I) oxidation. Using a concentration of 0.005 M for the diffusion limiting species in the mixed solution, the diffusion coefficient for Tl(I) in this solution was $2.0 \times 10^{-6} \text{ cm}^2/\text{s}$. Measured diffusion coefficients for Tl(I) and Pb(II) in individual solutions of 0.005 M TlNO_3 and 0.1 M $\text{Pb}(\text{NO}_3)_2$ in 5 M NaOH were 2.1×10^{-6} and $3.8 \times 10^{-7} \text{ cm}^2/\text{s}$, respectively.

The Cottrell equation is derived with the assumption that convective contributions to the current are negligible. Although this condition is usually satisfied by using an un-

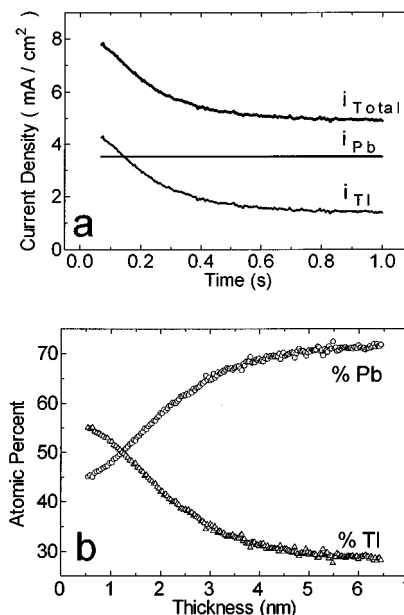


FIG. 3. Resolution of the observed current transient resulting from the 230 mV pulse into the current components due to Tl(I) and Pb(II) oxidation (a), and the Pb and Tl composition profiles in the superlattice layer calculated from these transients (b).

stirred solution, the solutions used to grow the superlattices in this study were stirred. We have found that the main effect of stirring is a nonzero intercept in the Cottrell plots. The measured diffusion coefficients using an unstirred solution were $2.6 \times 10^{-6} \text{ cm}^2/\text{s}$ for the mixed solution and 2.7×10^{-6} and $4.3 \times 10^{-7} \text{ cm}^2/\text{s}$ for the 0.005 M Tl(I) and 0.1 M Pb(II) solutions, respectively. The Tl(I) diffusion coefficient is a strong function of the NaOH concentration. It varies from $2.7 \times 10^{-6} \text{ cm}^2/\text{s}$ in 5 M NaOH to $1.9 \times 10^{-5} \text{ cm}^2/\text{s}$ in 1 M NaOH. The diffusion coefficient that we measure in 1 M NaOH is in good agreement with the literature value of $2.1 \times 10^{-5} \text{ cm}^2/\text{s}$ in the same solution.¹²

The composition profile in the 230 mV layer was calculated by assuming that the composition at a given time is directly proportional to the ratio of the currents due to the Pb(II) and Tl(I) oxidation, and that the current due to Pb(II) oxidation is constant throughout the pulse. The Pb(II) component of the total current was estimated from the steady-state current at long times and the known composition of bulk films grown at this potential. The steady-state current density at 230 mV is $4.6 \text{ mA}/\text{cm}^2$. Using the bulk concentration of 76% (metals only basis) for a film grown at 230 mV, the lead component of the total current density was calculated to be $3.5 \text{ mA}/\text{cm}^2$. The observed current and the calculated Pb(II) and Tl(I) components of the observed current as a function of time are shown in Fig. 3(A). The calculated lead and thallium concentration profiles are shown in Fig. 3(B). The layer thickness in Fig. 3(B) was calculated by integrating the current-time transient and applying Faraday's law.¹ Approximately $1.14 \mu\text{m}$ of material deposit for each C/cm^2 of anodic charge density. The lead content in the layer varied from 46% at 0.6 nm to 72% at 6.4 nm in the 230 mV layer, even though the applied potential-time waveform was square. We assume that the composition profile in the 70 mV

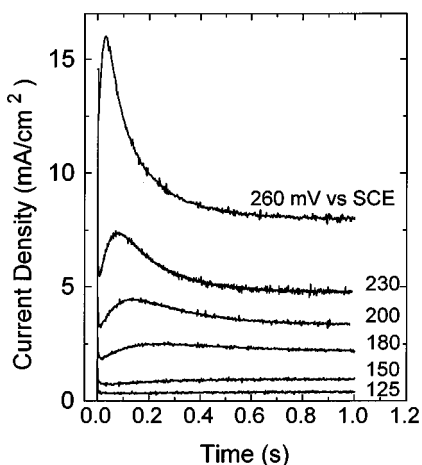


FIG. 4. Current-time transients for superlattices grown at a series of potentials. The scans were stepped to the potential shown from an applied potential of 70 mV vs SCE. At potentials below 150 mV vs SCE the depositions are kinetically controlled and the current-time transients are flat.

layer is flat, since both Tl(I) and Pb(II) oxidation are kinetically controlled at that potential.

The graded composition profile that we calculated for the high potential layer in the superlattice grown by pulsing the potential between 70 and 230 mV versus SCE may be desirable for some applications. For example, grading the composition and lattice parameter may inhibit misfit dislocation formation in strained-layer superlattices. In semiconductor devices for optical or electronic applications, however, it may be desirable to have square composition profiles.¹³ Our results indicate that as long as one component of the material is diffusion limited, it should not be possible to electrochemically grow superlattices with square composition profiles. One approach to circumvent this problem is to use a dual-bath deposition system.^{14,15} The approach we use, however, is to lower the potential of the high potential pulse so that both components of the layer are deposited under kinetic control.

The current-time transients following a potential pulse can be used to select the appropriate potentials so that both layers of the superlattice are grown under kinetic control. The transients in Fig. 4 were determined by pulsing from 70 mV to potentials ranging from 125 to 260 mV versus SCE. The transients become flat and do not show diffusionlike decays when the potential is lowered below about 150 mV versus SCE. Since both the applied potential time and measured current-time transients are flat at the potentials below 150 mV versus SCE we assume that the composition profiles are also square.

The calculated composition profiles are shown in Fig. 5 for three superlattices that were grown by pulsing between 70 mV and 150, 230, or 260 mV versus SCE. The composition of the 150 mV layer is relatively constant at 64 ± 3 at. % lead, while the lead content of the 260 mV layer varies from 39% to 76% through the layer. Since the composition of the

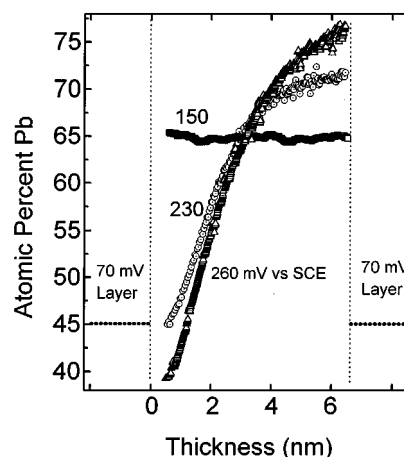


FIG. 5. Calculated composition profiles for superlattices grown by pulsing the potential between 70 mV and 150, 230, or 260 mV vs SCE.

70 mV layer is constant at about 45% lead, the interfaces that this layer forms with the 230 and 260 mV layers are highly asymmetrical.

The electrochemical method is ideal for both measuring and tailoring the interface symmetry and composition profiles of superlattices in real time on a subnanometer scale. Work is underway in our laboratory to compare the calculated composition profiles for these superlattices to the apparent height profiles obtained by cross-sectional STM,²⁻⁴ and to modulation functions calculated from the x-ray satellite intensities.

This work was supported in part by National Science Foundation Grant DMR-9202872, Office of Naval Research Grant N00014-91-J-1499, and the University of Missouri Research Board.

- ¹J. A. Switzer, M. J. Shane, and R. J. Phillips, *Science* **247**, 444 (1990).
- ²J. A. Switzer, R. P. Raffaele, R. J. Phillips, C.-J. Hung, and T. D. Golden, *Science* **258**, 1918 (1992).
- ³J. A. Switzer and T. D. Golden, *Adv. Mater.* **5**, 474 (1993).
- ⁴T. D. Golden, R. P. Raffaele, and J. A. Switzer, *Appl. Phys. Lett.* **63**, 1501 (1993).
- ⁵J. A. Switzer, C.-J. Hung, B. E. Breyfogle, M. G. Shumsky, R. Van Leeuwen, and T. D. Golden, *Science* **264**, 1573 (1994).
- ⁶U. Cohen, F. B. Koch, and R. Sard, *J. Electrochem. Soc.* **130**, 1987 (1983).
- ⁷D. Tench and J. White, *Metall. Trans. A* **15**, 2039 (1984).
- ⁸D. S. Lashmore and M. P. Dariel, *J. Electrochem. Soc.* **135**, 1218 (1989).
- ⁹Y. Yahalom, *J. Mater. Res.* **4**, 755 (1989).
- ¹⁰B. E. Breyfogle, R. J. Phillips, and J. A. Switzer, *Chem. Mater.* **4**, 1356 (1992).
- ¹¹A. J. Bard and L. R. Faulkner, *Electrochemical Methods* (Wiley, New York, 1980), p. 143.
- ¹²M. A. Bellavance and B. Miller, in *Encyclopedia of the Electrochemistry of the Elements*, edited by A. J. Bard (Marcel Dekker, New York, 1978) Vol. 13, p. 192.
- ¹³T. J. deLyon, H. C. Casey, P. M. Enquist, J. A. Hutchby, and A. J. Springthorpe, *J. Appl. Phys.* **65**, 3282 (1989).
- ¹⁴L. M. Goldman, B. Blanpain, and F. Spaepen, *J. Appl. Phys.* **60**, 1374 (1986).
- ¹⁵C. A. Ross, L. M. Goldman, and F. Spaepen, *J. Electrochem. Soc.* **140**, 91 (1993).